Supporting Information

Defects in the Amorphous-Crystalline Evolution of Gel-Derived TiO_2

C. Koral[†#], M. Fantauzzi[‡#], C. Imparato[§#], G. P. Papari[†f], B. Silvestri[§], A. Aronne[§], A. Andreone[†f], and A. Rossi[‡*]*

[†]*National Institute for Nuclear Physics, UdR Napoli, Via Cinthia, 80126 Napoli, Italy*

[‡]*Department of Chemical and Geological Science, University of Cagliari, S.S. 554 Bivio per Sestu, 09042 Monserrato, Cagliari, Italy*

[§]*Department of Chemical, Materials and Production Engineering, University of Naples Federico II, P.le V. Tecchio 80, 80125 Napoli, Italy*

[f]*Department of Physics, University of Naples Federico II, and CNR-SPIN, UOS Napoli, Via Cinthia, 80126 Napoli, Italy*

[#] These authors equally contributed to this investigation.

* *Corresponding authors*: antonello.andreone@unina.it; antonella.rossi@unica.it.

The X-ray diffraction patterns for the particulate (inorganic gel, SGT) and for the acetylacetonate-TiO_2 hybrid gel (HSGT) are shown in Figure S1 together with the patterns obtained following a thermal treatment at 400°C, 600°C and 800°C and for various heating time. Both gels are amorphous when dried in environmental conditions at 50 °C. Crystallization starts occurring into the anatase phase upon annealing at 400 °C. At 800 °C the anatase-rutile transition is complete in the case of HSGT while in the case of SGT 5% of anatase phase is still detected.

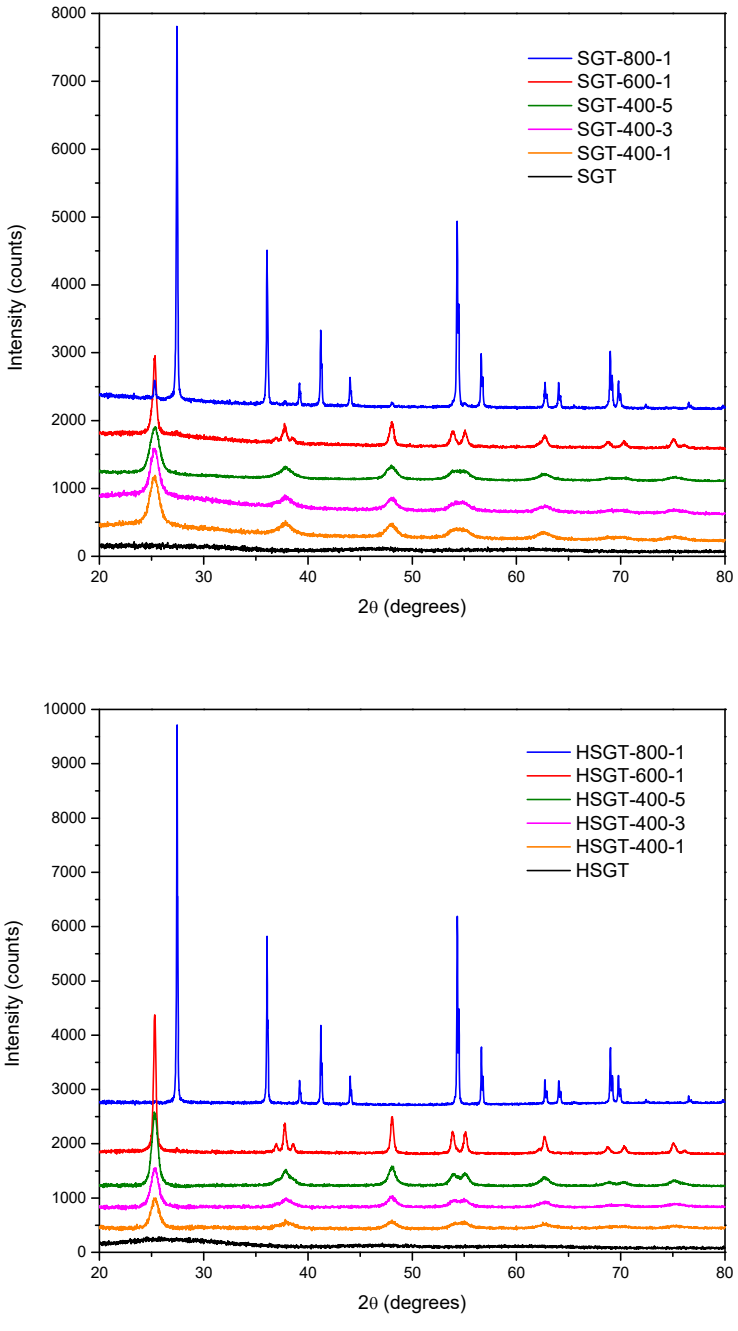

Figure S1: XRD patterns of all studied SGT and HSGT samples.

For the curve fitting of Ti 2p XPS peaks the components due to Ti (IV), Ti (III) and Ti sub-oxides are considered (Figure S2). The signals ascribed to reduced Ti species, which are expected to be at about 457 eV and 456 eV, are not detected.

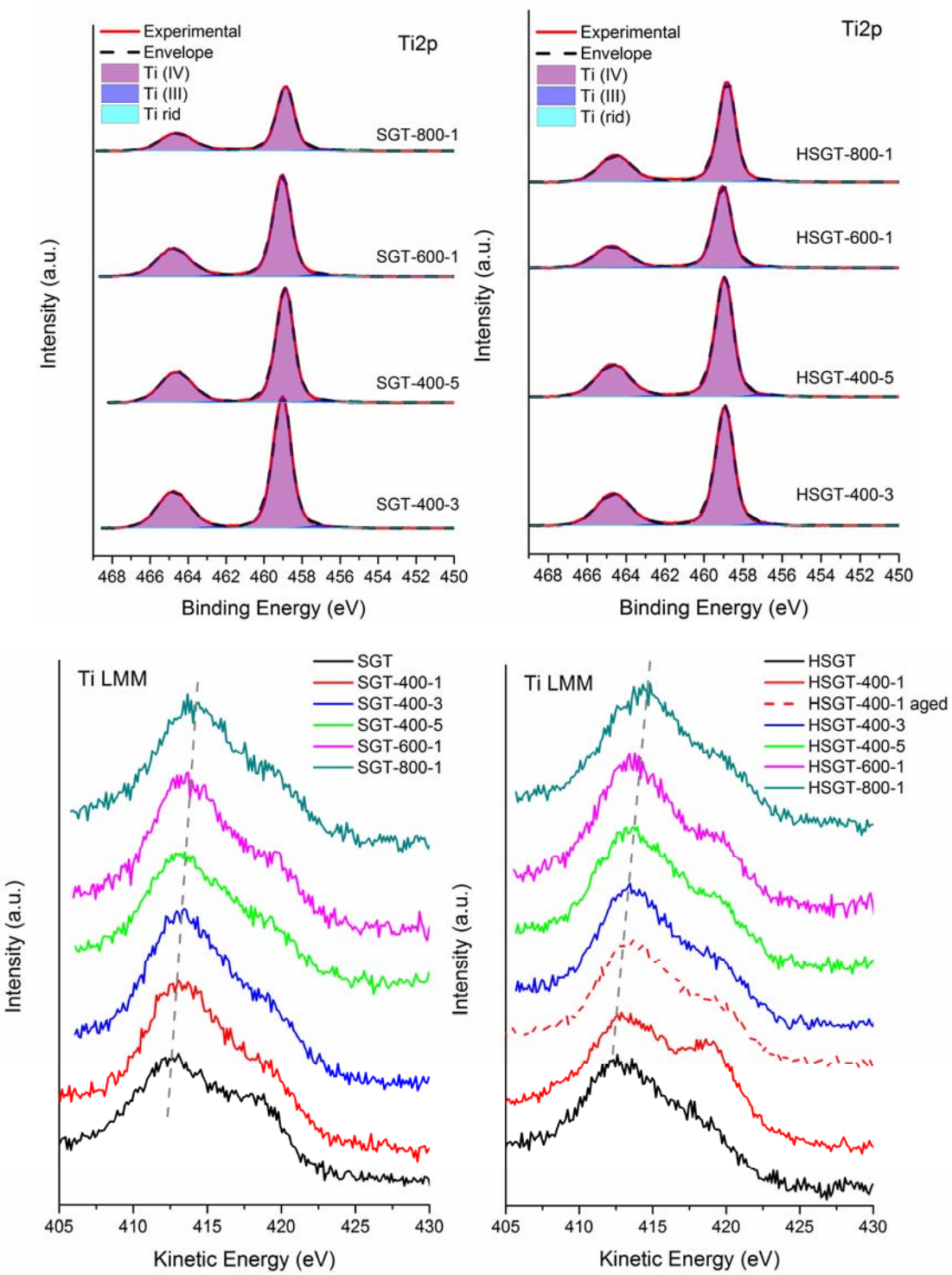

Figure S2. Ti 2p and Ti LMM XP - high-resolution spectra of SGT and HSGT samples.

An example of X-ray induced OKLL spectrum after background subtraction and curve fitting is provided in Figure S3. The Auger oxygen spectra were fitted with model functions constraining all parameters except the peak position and the peak intensity (area) to be able to calculate the peak separation between $KL_{23}L_{23}$ and O KL_1L_{23} difference and their ratio (Table S1). These two values are related to the bond Ti–O ionicity and the application to the samples of TiO_2 obtained with various treatments is explained in the main text; see Figure S4a and S4b for SGT and HSGT respectively.

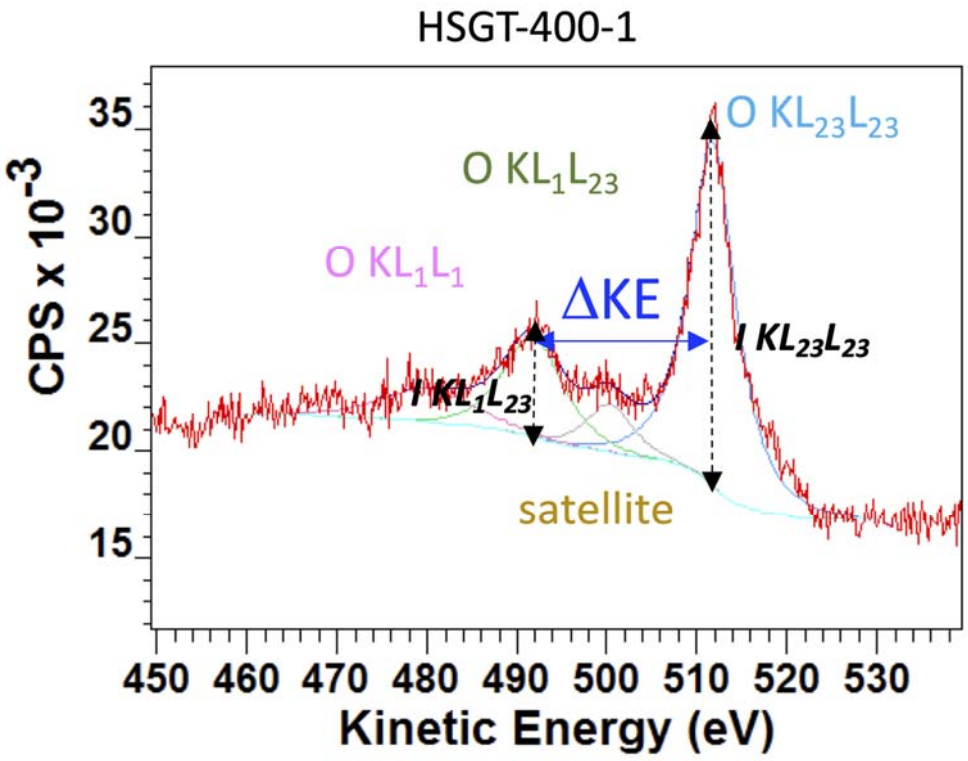

Figure S3. Example of O KLL X-ray induced Auger peak recorded on HSGT-400-1 sample

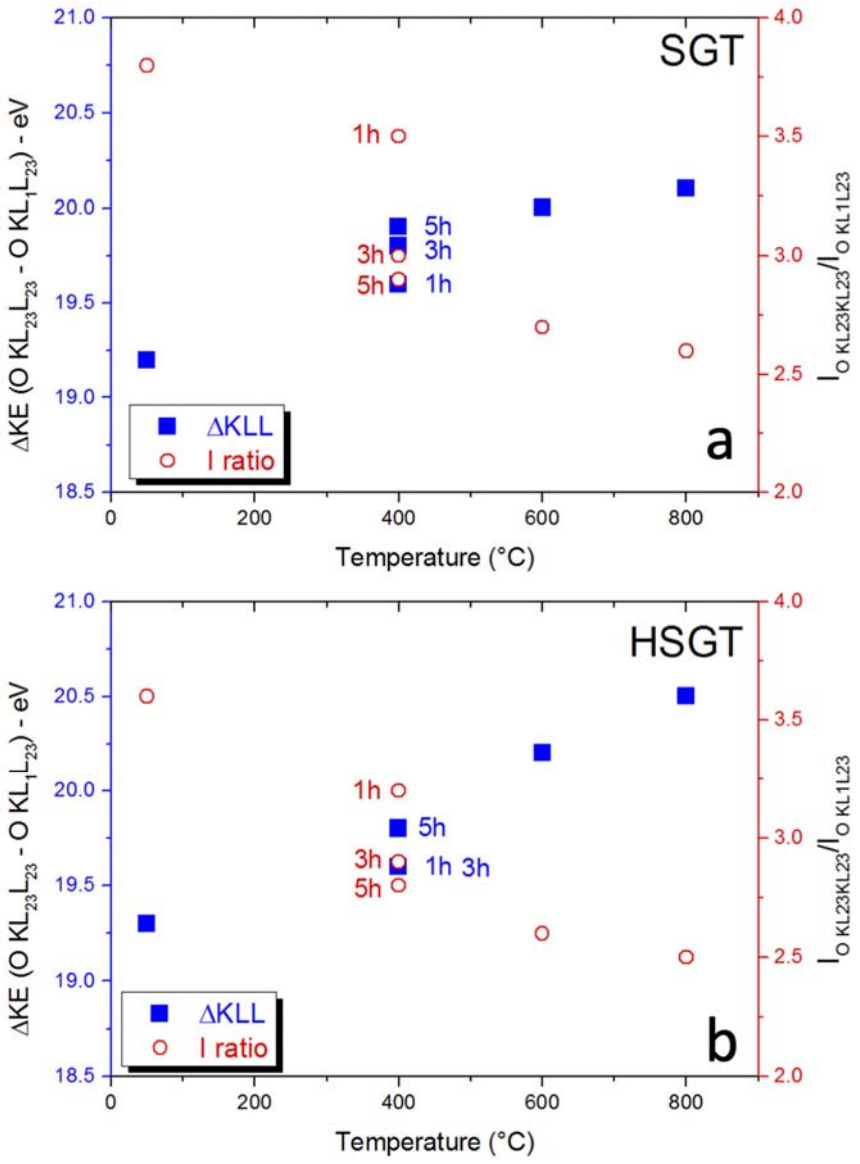

Figure S4: Kinetic energy differences (blue squares) and intensity ratios (red squares) between O $KL_{23}L_{23}$ and O KL_1L_{23} evaluated as a function of temperature for SGT (a) and HSGT (b) series.

To determine the presence of defects in the materials here investigated, the O1s spectrum (Figure S5) was fitted with model Gaussian-Lorentzian functions. The oxygen photoelectron signal is multicomponent for all the samples, showing the presence of O in TiO_2 at 530 eV, and of a component that might be ascribed to -OH and/or oxygen deficient regions at 531 eV. The third component was assigned to some adsorbed water (BE = 533 eV). The peak area of the second component at 531 eV was plotted versus the annealing temperature in Figure 6. The difference between the two series of samples SGT and HSGT is supporting that the component is mainly due to oxygen in defective sites in the case of HSGT.

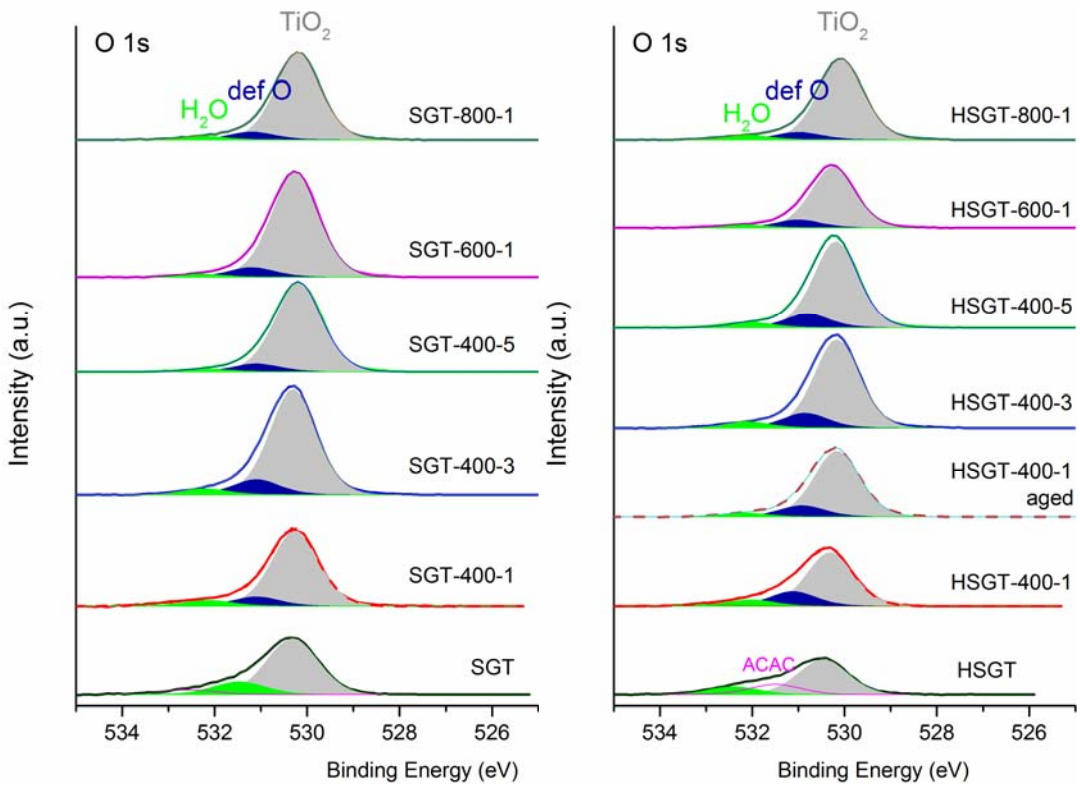

Figure S5. O 1s peaks recorded on the SGT and HSGT series.

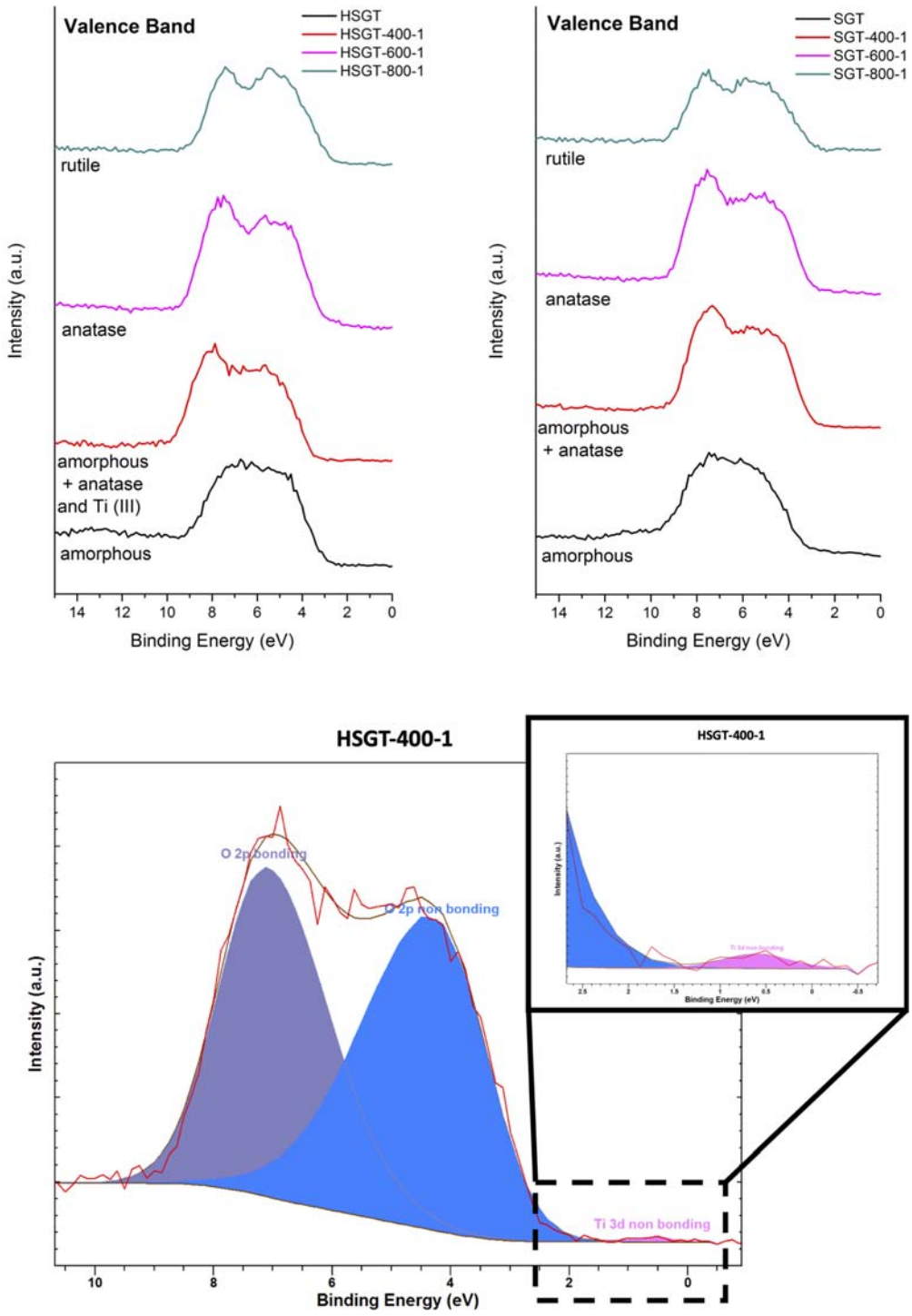

Figure S6. XPS valence band spectra recorded on HSGT and SGT samples.

Table S1. Kinetic energy (eV) of O $KL_{23}L_{23}$ and O KL_1L_{23}, energy separation (eV) and intensity ratio.

	Kinetic Energy (eV ± 0.1)		ΔKE (eV ± 0.2)	$I_{OKL23L23}/I_{OKL1L23}$
	O $KL_{23}L_{23}$	O KL_1L_{23}		
SGT	511.4	492.2	19.2	3.8 (0.1)
SGT-400-1	511.5	491.9	19.6	3.5 (0.2)
SGT-400-3	511.9	492.2	19.7	3.0 (0.1)
SGT-400-5	511.8	491.9	19.9	2.9 (0.1)
SGT-600-1	512.2	492.2	20.0	2.76 (0.01)
SGT-800-1	512.5	492.4	20.1	2.56 (0.07)
HSGT	510.8	491.5	19.3	3.6 (0.2)
HSGT-400-1	511.9	492.4	19.5	3.2 (0.2)
HSGT-400-1 aged	511.8	492.0	19.8	2.8 (0.1)
HSGT-400-3	511.8	492.1	19.8	2.8 (0.1)
HSGT-400-5	511.8	492.1	19.8	2.91 (0.05)
HSGT-600-1	511.5	491.3	20.2	2.62 (0.03)
HSGT-800-1	511.8	491.3	20.5	2.5 (0.1)